Available online at www.sciencedirect.com
SCIENCE DIRECT®
Simulation Modelling Practice and Theory 13 (2005) 437–449
SIMULATION MODELLING PRACTICE AND THEORY
www.elsevier.com/locate/simpat

An algorithm for simulating human arm movement considering the comfort level

Feng Yang *, Li Ding, Chunxin Yang, Xiugan Yuan

Institute of Human-Machine and Environment Engineering, Beijing University of Aeronautics and Astronautics, 37 Xueyuan Road, Haidian District, Beijing 100083, China

Received 15 January 2003; received in revised form 21 December 2004; accepted 29 December 2004
Available online 2 March 2005

Abstract

Seeking other joint trajectories of human arm in terms of given trajectory of hand is a wide research problem. In this paper, the computational problem of inverse kinematics of arm movement was investigated. On the basis of an eight-DOF arm model, an inverse kinematics algorithm recreating arm motion was developed in accordance with the human's feedback control mechanism of motor. In this method, the comfort level, an ergonomic index was adopted as the performance function of the motor control. Through maximizing the comfort level, human arm movement can be simulated when the end-effecter motion is given. This method combines human dynamics and ergonomics. To evaluate the approach, some arm goal-directed movement experiments were carried out. The joint trajectories were predicted with an average $R^2 = 0.9627$ and mean residual error MRE = 0.0094 m, which indicates that the presented algorithm provides a feasible method to simulate arm goal-directed movement and can be used as an efficient postural manipulation tool for the virtual reality.

Keywords: Arm movement; Simulation; Comfort level; Inverse kinematics; Inverse dynamics

* Corresponding author. Present address: Applied Health Building MC898, 1919 W. Taylor St., Chicago, IL 60612, United States. Tel.: +1 312 355 3988; fax: +1 312 996 4583.
E-mail address: yangf2050@yahoo.com (F. Yang).

1569-190X/$ - see front matter © 2005 Elsevier B.V. All rights reserved.
doi:10.1016/j.simpat.2004.12.004

1. Introduction

Virtual environment systems provide immersible visual displays of computer graphics, which can be widely used in many fields, such as entertainment, aerospace training, and industrial design. In these systems, a participant is connected to a synthetic human agent through appropriate sensors. With the aid of a real-time association between users joint or end-effecter positions and orientations, the corresponding parts of the synthetic agent are made to move in synchrony. In the virtual reality, what usually interests us is finding the joint angles from the end-effector's coordinates. Goal-directed movement, such as moving a hand along a given trajectory requires the computation of inverse kinematics, which solves for the set of joint angles from the end-effector's location and orientation. The problem, however, is ill-posed because the number of degrees of freedom (DOF) of the human body is generally greater than the number of equations imposed by the task. This means that there exit more than one possible solution for completing a task. There have been a considerable amount of interests and efforts dedicated to understanding of how humans control complex movements of upper limb in human behavioral sciences and for the need of simulations in computer animation and robotics [1–3].

Many previous attempts of human arm point-to-point reaching motion have focused on studying kinematic and kinetic profiles during voluntary movements, which depend upon a large amount of experiments [4,5]. By means of mathematic tools, such as statistics and regression to experimental data, some conclusions have been consistently yielded. One limitation of these mathematical modeling techniques, however, is that they leave little room for further and physical interpretation. Furthermore, the motions of subjects' hands were constrained in either the vertical plane or the horizontal plane in these works.

Some other researchers employed inverse kinematics and inverse dynamics to study the movement of the arm. Tolani et al. [6] developed a fast algorithm on the basis of a combination of analytical and numerical methods. This set of inverse kinematics algorithms is suitable for an anthropomorphic arm or leg. To find a solution of the inverse kinematics problems of robot manipulators, Hollerbach et al. [7] used optimization with emphasis on the accomplishment of a motion within constraints and optimizing it by some criteria such as time, torque, energy and obstacles. Inspired by the above studies, many researchers in bioengineering have proposed methods to calculate the human motion by minimizing some physical values, such as the jerk, torque change, muscle force change, muscle signal change, and kinetic energy by joints. Koga et al. [8] created a motion planning system of the arms that can move objects from one position to another. However, the underneath motor control system between human and robotics is strikingly different. The bases of above algorithm are mainly robotics dynamics and kinematics, with little or consideration of human character.

Lo developed a fast recursive dynamics algorithm for dynamically simulating articulated 3D human models based on minimizing the joint torque in the course

of motion [9]. This approach takes the absolute value of torque as the standard of the comfort level. However, there is obviously a limit of torque that can be generated at a joint. Whether human feel comfortable or not depends on the relative value rather than the absolute joint torque. Lee et al. [10] controlled the arms of a human body model by determining the direction of the hand movements according to the comfort level. The comfort level of each joint was calculated by the following equation at each moment:

$$\mathrm{cl} = \frac{\tau_{\max} - \tau}{\tau_{\max}} = 1 - \frac{\tau}{\tau_{\max}} = 1 - \mathrm{dcl} \tag{1}$$

where cl and dcl are the comfort level and discomfort level of a joint, respectively. τ represents the torque exerted by the joint, and $\tau_{\max}$ is the maximum torque the joint can produce, which is obtained from the ergonomics data. Their approach established the architecture of human motion control system including condition monitor, path planning scheme, and rate control process. It can automatically generate the motion path when the initial and ending position of human body are given. Though the algorithm could simulate the arm movement, it was too complex to be used in the virtual reality as real-time application. In addition, it cannot obtain the joint trajectories when the trajectory of the end effecter is given.

The introduction of comfort level is based on the motion control mechanism of human body. Human bodies are loaded with sensors that feedback information to the central nervous system regarding our internal state and the environment around us. In general, this information is utilized to affect ongoing control strategies and suggests a role for feedback. At any moment of the human motion, when the force or torque exerted by muscle group at the joint are close to the maximum torque the joint can produce, human can feel the discomfort although he does not exactly know the value of the torque he exerted. Then the degree of difficulty about accomplishing the next phase work can be predicted. The effecter organs undertaking work feel intense, which will in turn lead to the cerebrum making motion commands to regulate the motion of muscle and control body position and orientation. The new configuration of body can supply more force and reduce the discomfort level of body. For example, the joints that have more available strength could undertake more load, whereas, those joints that have less usable strength undertake less load. If it is difficult to accomplish the motion with the present joints, some other joints will be added to share the excessive joint torque with other joints in order to reduce the workload of the joints. In general, with the own feedback control mechanism, human always keep the joints at a high comfort level, that is to say human tend to operate within a comfort region, which is the basis of the algorithm presented in this paper.

In present study, we proposed an algorithm based on the combination of inverse kinematics, inverse dynamics, and biomechanical information. The comfort level cl of human arms, which demonstrates the ergonomics of human body, is adopted to control and plan the motion path of human multi-joint arms.

2. Arm model

2.1. Geometric models

The system of articulated links connected by rotary joints are adopted to illustrate the human arm in this study. The arm is described as a system consisting of four segments: the trunk, the upper arm, forearm and hand. The upper arm is connected to the trunk by a ball-and-socket joint; the lower arm is connected to the upper limb by a two-DOF joint; the hand is connected to lower arm by a ball joint. The shoulder and wrist have three DOFs while the elbow is a two-DOF joint. Then, the arm is a four-segment, eight-DOF, and two degree of redundancy rigid body system.

The arm can be represented topologically using a kinematic chain structure in which links represent arm segments. The trunk is considered as the root of the chain, and the outmost link, the hand is its leaf. Two links connected by a joint are the parent and child links of the joint, depending on whether the link is more proximal or distal to the root. The joint is called the root joint of its child link. Each link has dynamic properties, such as mass, the center of mass, the principal inertial matrix, and the rotation matrix from the link's root joint coordinate frame to its local coordinate frame.

For the sake of simplifying the following calculation, we apply standard robotics techniques, Denavit–Hartenberg notation (DH-notation) [11], which describes the coordinate transformation from distal link L_i to proximal link L_{i+1} using a 4×4 transformation matrix $\mathbf{A}_{i,i+1}$. Once a linked system is represented in this form, its kinematics is computable in a systematic way. However, DH-notation is only designed for a system with single DOF joints. In order to use the DH-notation, it is necessary that transforming the arm into a system connected by single DOF joints. The method proposed by Huang et al. [12] is used to transform the human arm. According to the method, the multi-DOF joint can be transformed into some consecutive single DOF joints by means of adding dummy links into a multiple-DOF joint. The dummy link is defined as the link without length, mass, and inertia. While, between the two consecutive generated single DOF joints there is a transformation matrix that describes the transformation relationship between the two new joint local coordinates. Therefore, three successive single degree freedom joints with two dummy links will replace a three DOF joint. The transformation of human arm is illustrated in Fig. 1. In this figure, the upper and lower parts are the geometric schemes of human arm before and after transformation respectively. For the upper part, the number in brackets near the joint is the number of the joint DOF. For the lower part, the joint J1, J2, J3 and dummy link L1, L2 make the shoulder joint; J4, J5 and dummy link L4 represent elbow joint; J6, J7, J8 and dummy link L6, L7 describe the wrist joint. L3 represents the upper arm and L5 the forearm.

2.2. Muscle strength model

Ultimately, the trajectory of an end-effecter is derived from the body's resource-strength: the maximum achievable joint torque. During the process of human

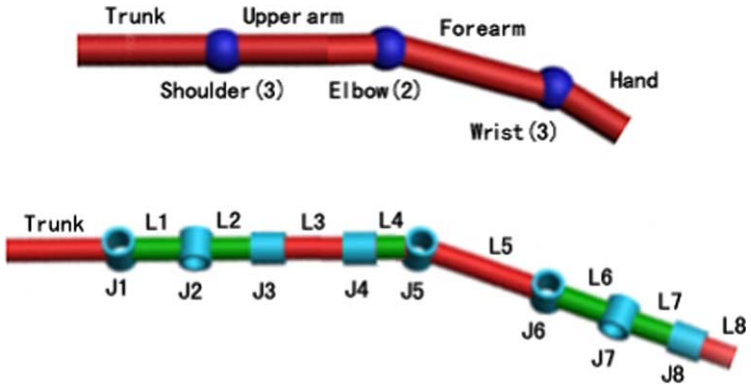

Fig. 1. The conversion scheme from multi-DOF joint to consecutive single-DOF joints of upper limb. The upper and lower parts are the geometric structures of the arm before and after transformation, respectively. For the upper part, the number in brackets near the joint is the number of the DOF corresponding to the joint. For the lower part, the joint J1, J2, J3 and dummy link L1, L2 compose the shoulder joint; J4, J5 and dummy link L4 represent elbow joint; J6, J7, J8 and dummy link L6, L7 describe the wrist joint. L3 represents the upper arm and L5 the forearm. The rotation axis of every single-DOF joint corresponds to one of the axes in the multi-DOF joint.

activities, the extension and shrink of muscles linking the bones create the torque at each joint. Strength (maximum torques) is defined as muscle group's strengths and is stored on a joint DOF basis. Modeling strength in terms of muscle group strength allows different people to possess different strength capacities in different muscle groups. Each DOF of a joint has two joint movements, which are associated with two different muscle groups. For example, the elbow has two DOFs, flexion/extension and pronatino/supination. Whereas, the shoulder and wrist have three rotational axes, i.e. they have three rotational directions. These three DOFs in the shoulder can be attributed to abduction/adduction, flexion/extension, and lateral/medial rotation. As for wrist, the three DOFs are the pronation/supination, flexion/extension, and radial/ulnar rotation. For each rotation axis of joints, there are two limits: one for extension and the other for flexion, which are determined from strength data.

In present study, when we study the force that leads to the movement of human arm, we do not concern on which specific muscle produces the force but the integral effects the muscles group produce in the movement. The strength of each muscle group is modeled as a function of body position, angular velocity, and other strength parameters. Pandya and Hasson [13] collected strength data for several human subjects. The strength testing was done using a special isokinetic dynamometer that limits the joint move along a singular DOF in every test. Strength varies with each individual and depends on joint angles and their angular velocity; it is approximated by a second-order polynomial,

$$\tau_{\max} = a_0(\dot{q}) + a_1(\dot{q})q + a_2(\dot{q})q^2 \tag{2}$$

where $\tau_{\max}$ is the maximum joint torque corresponding to specific rotation angle of joints, q; a_0, a_1, and a_2 present the regression parameters, which depend on the rotation direction and angular velocity of upper limbs, $\dot{q}$. In this model, one expression specifically represents the strength at one DOF for a given joint.

3. Methods

3.1. Inverse dynamics

The force and torque at each joint during motion can be calculated with the generalized coordinate parameters of the body. This operation is called inverse dynamics. To explore the power of computer graphics and animation in multi-segment dynamic system analysis, Kane and his associates have developed a particularly efficient multi-body dynamics equation formulation method. An outgrowth of their work is the development of highly efficient algorithms for multi-body analysis that have been incorporated in the computer program. Hence, Kane's method is used to determine joints forces and torques in this paper.

In general, the motion equations [14] in the form of Kane's method of the multi-body system, which includes β segments and possesses N DOFs, are formulated as:

$$\mathbf{M}\dot{\mathbf{u}} = \mathbf{F} \tag{3}$$

where $\mathbf{M} \in \Re^{N\times N}$ is a positive definite mass matrix, $\mathbf{F} \in \Re^{N}$ is a force vector which includes the contribution of inertial forces and active forces, and $\mathbf{u} \in \Re^{N}$ Kane's generalized velocities. Kane's method utilizes the following highly efficient formula to obtain the mass matrix elements:

$$m_{rs} = \sum_{k=1}^{\beta} \left[m_k \mathbf{v}_{pk}^{(r)} \mathbf{v}_{pk}^{(s)} + \left(\mathbf{I}_k \boldsymbol{\omega}_{pk}^{(s)} \right) \boldsymbol{\omega}_{pk}^{(r)} \right] \quad r, s = 1, 2, \ldots, N \tag{4}$$

In this equation, m_k and $\mathbf{I}_k$ represent the mass and central inertia dyadic of body k, respectively. The vector quantities $\mathbf{v}_{pk}^{(s)}$ and $\boldsymbol{\omega}_{pk}^{(r)}$ are Kane's partial linear velocities and partial angular velocities for body k, respectively.

3.2. Inverse kinematics

Basically, the inverse kinematics technique consists of determining the rotations sequence of an articulate chain given the Cartesian position and orientation of its end-effecter with respect to the reference coordinate system. Inverse kinematics is a non-linear mapping from workspace to joint space.

The velocity of the center of mass of hand, $\dot{\mathbf{X}} \in \Re^6$ which includes the linear velocity $\mathbf{v} \in \Re^3$ and angular velocity $\boldsymbol{\omega} \in \Re^3$ of the endpoint, can be given by

$$\dot{\mathbf{X}} = \mathbf{J}\dot{q} \tag{5}$$

where $\mathbf{J} \in \Re^{6\times N}$ is a Jacobian matrix which provides the geometrical relationship between the endpoint coordinate system referenced to an inertial frame of reference, and the joint coordinates referenced to the inboard joint's coordinate frame. $\mathbf{J}$ includes two parts, $\mathbf{J}_A$ and $\mathbf{J}_L$ corresponding with angular and linear transformation, respectively. $\mathbf{q} \in \Re^N$ indicates the vector of joint angle.

To non-redundant system, the $\dot{\mathbf{q}}$ can be calculated through solving Eq. (5). Then, integrating and differentiating the $\dot{\mathbf{q}}$ respectively, we can obtain the angular displacement $\mathbf{q}$ and angular acceleration $\ddot{\mathbf{q}}$. However, for humans arm, a kind of redundant system, we have to resort to some other optimization algorithm. Gradient projection method is a widely used method. Its essential expression [15] is:

$$\dot{\mathbf{q}} = \mathbf{J}^{+}\dot{\mathbf{X}} + \alpha(\mathbf{I} - \mathbf{J}^{+}\mathbf{J})\nabla H \tag{6}$$

where $\mathbf{J}^{+} \in \Re^{N\times 6}$ is called the pseudo inverse matrix of $\mathbf{J}$, α is an arbitrary constant, $\mathbf{I} \in \Re^{N\times N}$ is an identity matrix in joint space, ∇H is the gradient of the performance function $H(\mathbf{q})$ at $\mathbf{q}$, $\nabla H = \partial H(\mathbf{q})/\partial \mathbf{q}$.

We concentrate on building up the control algorithm based on the optimization of the comfort level. According to Eq. (1), the sum of comfort level and discomfort level equals one. Maximizing cl and minimizing dcl is akin. Thus the problem can be changed into minimizing dcl. To identify the discomfort level of entire arm, we choose the maximum one, dcl^*, from all discomfort level of the arm system,

$$\mathrm{dcl}^* = \max_{1\leqslant i\leqslant N}\{(\mathrm{dcl})_i\} \tag{7}$$

The dcl^* is selected as the performance function for the gradient projection method. So Eq. (6) can be rewritten as follows,

$$\dot{\mathbf{q}} = \mathbf{J}^{+}\dot{\mathbf{X}} + \alpha(\mathbf{I} - \mathbf{J}^{+}\mathbf{J})\nabla(\mathrm{dcl}^*) \tag{8}$$

If the kinematics parameters of the end-effecter are specified, then $\mathbf{q}$ can be obtained by integrating the above equation.

4. Experiments

We select the goal-directed movement of arm as the simulated example. The trajectory of hand has been given, and then our algorithm will be applied to calculate the kinematics parameters such as angle, angular velocity and angular acceleration of wrist and elbow.

An orthogonal axis system, as the referenced frame of the entire arm, is defined by the intersection of the three principal planes of the body passing through the center of shoulder as shown in Fig. 2. The z-axis is formed by the intersection of the sagittal plane and the frontal plane; the y-axis, by the intersection of the frontal and transverse planes; and the x-axis by the intersection of sagittal and transverse planes.

The shoulder or wrist joint can be transformed into a three single DOF joints chain and the elbow can be represented by two single DOF joints. The rotation axis of every single DOF joint is determined by the physical direction of joints. Based on

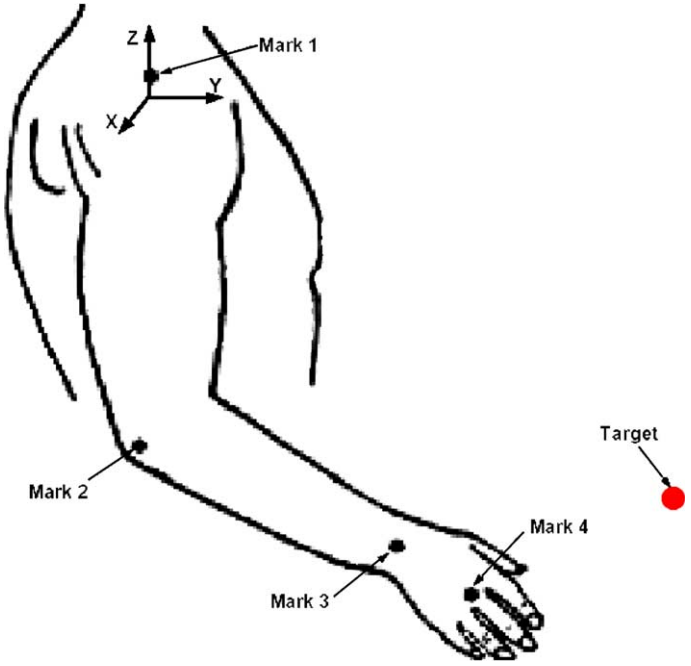

Fig. 2. The scheme of the experimental setup and coordinates system. Subjects sat on a stable chair with the trunk strapped to the chair back and kept the trunk from moving when he was reaching a goal indicated by a red ball. Four markers covered with reflecting material, were placed on the shoulder (acromion), elbow (lateral epicondyle), wrist (cubitus styloid process), and hand (the metacarphphalangeal joint of middle finger). The z-axis is defined by the intersection of the sagittal plane and the frontal plane; the y-axis, by the intersection of the frontal and transverse planes; and the x-axis by the intersection of sagittal and transverse planes.

the DH-notation, using homogeneous transformations **A** matrix, which is the function of the joint variable **q**, the transformation matrix, $\mathbf{T} \in \Re^{4\times4}$ from the shoulder coordination frame to hand coordination frame is,

$$\mathbf{T} = \mathbf{A}_{0,1}\mathbf{A}_{1,2}\cdots\mathbf{A}_{N-1,N} \tag{9}$$

Actually, **T** represents the spatial position and orientation of the hand in the base coordination frame. Furthermore, the Jacobian can be computed using the following equation,

$$\begin{aligned} \mathbf{J}_{\mathrm{L},j} &= \frac{\partial \mathbf{T}(i,4)}{\partial q_j} \quad i = 1,2,3 \\ \mathbf{J}_{\mathrm{A},j} &= \mathbf{b}_{j-1} \quad j = 1,2,\ldots,N \end{aligned} \tag{10}$$

where j is the column number in the Jacobin matrix, $b_{j-1} \in \Re^3$ represents the joint axis $j-1$ with reference to the base coordinate system.

Using the trajectory of the end-effecter and the following equation, we can attain the velocity of end point, $\dot{\mathbf{X}} = [\mathbf{v}\ \boldsymbol{\omega}]^{\mathrm{T}}$,

$$\begin{aligned} \mathbf{v} &= \Delta x/\Delta t \\ \boldsymbol{\omega} &= -\widehat{\mathbf{r}}^{-1}\mathbf{v} \end{aligned} \tag{11}$$

where $\mathbf{r} = [r_x\ r_y\ r_z]$ is the position vector to the centroid of hand in the base coordinate system. $\widehat{\mathbf{r}}^{-1} = \begin{bmatrix} 0 & -r_z & r_y \\ r_z & 0 & -r_x \\ -r_y & r_x & 0 \end{bmatrix}$ is the inverse matrix of $\widehat{\mathbf{r}}$. To avoid accumulating deflection produced by linear model at time step of t^m, $\mathbf{x}^m$ should be substituted with $\widetilde{\mathbf{x}}^m$ that can be obtained utilizing equation, $\widetilde{\mathbf{x}}^m = \mathbf{J}\mathbf{q}^m$. The superscript m denotes the mth time step. Then, Eq. (11) is rewritten as:

$$\begin{aligned} \mathbf{v}^m &= (\mathbf{x}^{m+1} - \widetilde{\mathbf{x}}^m)/\Delta t \\ \boldsymbol{\omega}^m &= (-\widehat{\mathbf{r}}^{-1})\mathbf{v}^m \end{aligned} \tag{12}$$

It is important to note that, since $\mathbf{J}$ varies with the orientation of the arm, a consequence for computer simulation is that terms of the matrix must be recalculated for each time interval during arm movement. Substitute the $\nabla(\mathrm{dcl}^*)$ and $\dot{\mathbf{X}}$ into Eq. (8); it can be rewritten at a finite difference approximation using explicit difference scheme as follows:

$$\mathbf{q}^{m+1} = \mathbf{q}^m + (\mathbf{J}^+)^m \begin{bmatrix} \mathbf{v}^m \\ \boldsymbol{\omega}^m \end{bmatrix} + \alpha(\mathbf{I} - (\mathbf{J}^+)^m\mathbf{J}^m) \begin{bmatrix} \frac{(\mathrm{dcl}^*)^m - (\mathrm{dcl}^*)^{m-1}}{q_1^m - q_1^{m-1}} \\ \frac{(\mathrm{dcl}^*)^m - (\mathrm{dcl}^*)^{m-1}}{q_2^m - q_2^{m-1}} \\ \cdots \\ \frac{(\mathrm{dcl}^*)^m - (\mathrm{dcl}^* d)^{m-1}}{q_N^m - q_N^{m-1}} \end{bmatrix} \Delta t \tag{13}$$

Using the trajectory of hand tested in experiment, we can calculate the kinematical parameters of elbow and wrist, such as angular displacement and angular velocity.

Six young adults (six males; range from 22 to 28 years of age) volunteered to serve as the subjects. All subjects were right-hand dominant and reported any neurological or muscular discomfort of abnormality at experiments. As depicted in Fig. 2, subjects were seated in a rigid chair with their trunk strapped to the chair back with a wide belt. Each subject was requested to reach a target lying in front of him only through moving his arm, i.e. the subject torso keep the initial configuration at experiments. Four markers (plastic sphere of 1.8 cm in diameter) covered with reflecting material, were placed on the shoulder (acromion), elbow (lateral epicondyle), wrist (cubitus styloid process), and hand (the metacarphphalangeal joint of middle finger). Movements of arms were recorded and analyzed by a motion analysis system at 240 Hz (Qualysis, Sweden). Marker paths were low-pass filtered at a specific cut-off frequency using recursive, fourth-order Butterworth filters.

Using the trajectory of hand (marker 4), we can obtain the linear and angular velocity of the end-effecter. In addition, the experimental conditions allow us to acquire the initial angle and angular velocity of every link. In each time interval, **J** and $\mathbf{J}^+$ can be calculated according to the geometrical configuration of the arm using Eq. (10). Selecting the joint angular velocities as the generalized velocity of the arm, we can attain the partial velocity and partial angular velocity of every segment related to the generalized velocity. Then joints torque can be calculated by Eq. (3). Having gained the maximum torque of the joints through Eq. (2), we can acquire the comfort level utilizing Eq. (1). Finally, the joints angle at the next time step can be solved through solving Eq. (13). Repeating this process until all time nodes are finished, the joints angle vector during the entire motion can be obtained. Using the forward kinematics, the trajectories of the elbow and wrist can be calculated.

To make a comparison, a coefficient of determination (R^2) was used to indicate the closeness of fit between estimated and measured results, and the mean residual error (MRE) to indicate the magnitude of the error. The algorithm predicated joint spatial position with a mean (SD) R^2 of 0.9627 ± 0.0393 across all subjects and joints (Table 1). MRE of these predictions was 0.0094 m (Table 1). The good agreement between actual and estimated results indicates the calculated orientation of end-effecter is accurate with respect to the measured orientation. As stated earlier, there are some others performance functions adopted to simulate arm movement. We selected the minimum torque method [7] to compared with the presented method. The calculation result showed the average R^2 of the minimum torque method was only 0.8704 ± 0.0862 and the MRE 0.0167 m for the same motions. Fig. 3 illustrates

Table 1
Summary of algorithm predictions of joints (the elbow and wrist) trajectories during arm movements

Subject	Joint	R^2			MRE (m)		
		X	*Y*	*Z*	*X*	*Y*	*Z*
1	Elbow	0.9428	0.9720	0.8247	0.0077	0.0105	0.0110
	Wrist	0.9684	0.9721	0.9707	0.0045	0.0086	0.0077
2	Elbow	0.9736	0.9637	0.9770	0.0153	0.0173	0.0132
	Wrist	0.9628	0.9796	0.9630	0.0053	0.0176	0.0090
3	Elbow	0.9826	0.9769	0.8278	0.0073	0.0149	0.0224
	Wrist	0.9853	0.9823	0.9778	0.0037	0.0075	0.0164
4	Elbow	0.9822	0.9770	0.9628	0.0022	0.0170	0.0076
	Wrist	0.9820	0.9827	0.9827	0.0064	0.0048	0.0113
5	Elbow	0.9761	0.9623	0.9720	0.0076	0.0121	0.0084
	Wrist	0.9745	0.9873	0.9867	0.0061	0.0056	0.0031
6	Elbow	0.9844	0.9709	0.8643	0.0113	0.0101	0.0096
	Wrist	0.9687	0.9651	0.9741	0.0034	0.0043	0.0068
Mean		0.9736	0.9743	0.9403	0.0067	0.0108	0.0105
SD		0.0121	0.0080	0.0622	0.0036	0.0049	0.0050

Mean and standard deviations are given for the 12 joints of 6 subjects.
MRE (m) = mean residual error.

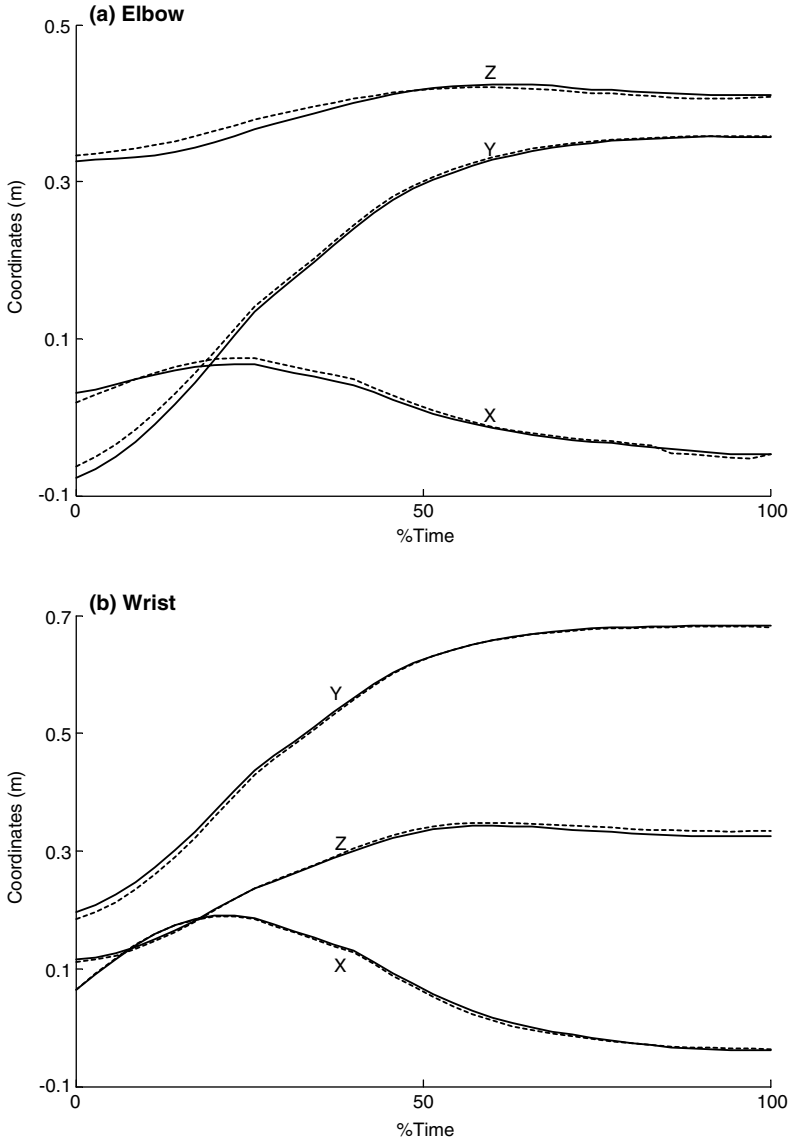

Fig. 3. Comparison of model estimated (dash lines) and measured (solid lines) trajectories of the joint of elbow (a) and wrist (b) for subject 1. R^2 and RMS are 0.9132 and 0.0097 m, 0.9704 and 0.0069 m for the elbow and wrist, respectively. The time was normalized by the whole movement time of arm.

the ability of the algorithm to well predict joint positions for a single subject. In this figure, the solid and dash lines represent the measured and estimated results, respectively.

5. Conclusions

A new algorithm for simulating human arm movement is developed and evaluated for its performance. Based on the experimental evaluation, the method allowing for human characters can produce reasonable and accurate arm motions. It can avoid the potential violation between human position and strength induced by sole inverse kinematics. Moreover, the kinematics of the human arm in terms of rotation angles in the joints is reconstructed from the spatial tracking system recordings. Therefore, this algorithm provides an effective method to recreate human animation, so it can be used in the virtual reality field to recovery human arm motion in real time.

From Table 1, the mean error between actual and estimated results is less than 1 cm. There are some sources can lead to this error. One is the anthropometrical parameter, such as errors of lengths of upper arm, forearm, hand, etc. The other is the measurement error coming from the motion capture system. Finally, the maximum joint torques calculated using regression equation (2) also generated some errors. In the future, we will perform the analysis to reduce these errors. For instance, we can precisely measure the studied subject's anthropometrical parameter with the aid of some professional measurement tools rather than using the regression equation [16] to estimate body parameters.

Acknowledgments

The support of the National High Technology Research and Development Program of China (863 Program) through the grant 2002AA743032 made this work possible and it is gratefully acknowledged. We would like to thank Haiting Cui, Jianming Huang, Xiaohong Gui, Minjing Sang, and Xin Xu for their contributions to the experiments. We also appreciate Lijing Wang and Yinxia Li for their helpful comments related to the work.

References

[1] T. Flash, N. Hogan, The coordination of arm movements: An experimentally confirmed mathematical model, Journal of Neuroscience 5 (1985) 1688–1703.
[2] E. Digby, B. Gordon, H. Matthew, The control of goal directed limb movements: Correcting errors in the trajectory, Human Movement Science 18 (1999) 121–136.
[3] N.-F. Yang, M. Zhang, C.-H. Huang, Synergic analysis of upper limb target-reaching movements, Journal of Biomechanics 35 (2002) 739–746.
[4] C. Papaxanthis, T. Pozzo, P. Stopley, Effects of movement direction upon kinematic characteristics of vertical arm pointing movements in man, Neuroscience Letters 253 (1998) 106–130.
[5] X.-D. Zhang, D.B. Chaffin, The effects of speed variation on joint kinematics during multisegment reaching movements, Human Movement Science 18 (1999) 741–757.
[6] D. Tolani, A. Goswnmi, N.I. Badler, Real-time inverse kinematics techniques for anthropomorphic limbs, Graphical Models 62 (2000) 353–388.

[7] J.M. Hollerbach, K.C. Suh, Redundancy resolution of manipulators through torque optimization, in: Proceedings of the International Conference on Robotics and Automation, 1985, pp. 1016–1021.
[8] Y. Koga, K. Kondo, J. Kuffner, Planning motions with intentions, Computer and Graphics 28 (1994) 395–408.
[9] J. Lo, Recursive dynamics and optimal control techniques for human motion planning, PhD thesis, Mechanical Engineering and Applied Mechanics, University of Pennsylvania, 1998.
[10] P. Lee, S.-S. Wei, J.-M. Zhao, Strength guided motion, Computer and Graphics 24 (1990) 253–262.
[11] J. Demavit, R.S. Hartembert, Kinematic notation for lower pair mechanism based on matrices, ASME Journal of Applied Mechanics (1955) 215–221.
[12] G. Huang, D. Metaxas, J. Lo, Human motion planning based on recursive dynamics and optimal control techniques, in: Proceedings of Computer Graphics International Conference, Geneva, 2000, pp. 19–28.
[13] A.K. Pandya, S.M. Hasson, Correlation and prediction of dynamic human isolated joint strength from lean body mass, N92-26682, 1992.
[14] D.E. Rosenthal, M.A. Sherman, High performance multibody simulation via symbolic equation manipulation and Kane's method, The Journal of the Astronautical Sciences 34 (1986) 223–239.
[15] W. Maurel, D. Thalmann, Human shoulder modeling scapulo-thoratcic constraint and joint sinus cones, Computer and Graphics 24 (2000) 203–218.
[16] P.D. Leva, Adjustment to Zatsiorsky–Seluyanov's segment inertia parameters, Journal of Biomechanics 29 (1996) 1223–1230.